CIB-W18/35-7-5

INTERNATIONAL COUNCIL FOR RESEARCH AND INNOVATION IN BUILDING AND CONSTRUCTION

WORKING COMMISSION W18 - TIMBER STRUCTURES

JOINTS WITH INCLINED SCREWS

I Bejtka

H J Blaß

Universität Karlsruhe (TH)

GERMANY

MEETING THIRTY-FIVE

KYOTO

JAPAN

SEPTEMBER 2002

Joints with Inclined Screws

I. Bejtka, H. J. Blaß - Universität Karlsruhe (TH), Germany

1 Introduction

Screws, bolts and dowels loaded perpendicular to the fastener axis are dowel-type fasteners, whose load-carrying capacity in timber-to-timber connections may be determined based on Johansen´s yield theory (Johansen, 1949). The ultimate load of joints with dowel-type fasteners loaded perpendicular to the fastener axis is limited by the embedding strength of the timber members and the bending capacity of the fasteners.

Exploiting the withdrawal capacity of long screws with continuous threads leads to increased load-carrying capacities and hence more economic connections. In order to increase the load-carrying capacity in timber-to-timber connections, the screws are not placed perpendicular to the interface between the members to be connected but arranged under an angle between 75° and 40° between the screw axis and the grain direction. The ultimate load of joints with inclined screws is then limited by the embedding strength of the timber members, the bending capacity and the withdrawal capacity of the fasteners as well as the friction between the timber members. Principally the screw is loaded in tension and the contact surface between the members in compression.

This paper compares the test results of connections with inclined screws and with fasteners loaded perpendicular to their axis. A proposal for design rules for single-shear joints with inclined screws is presented.

2 Timber-to-timber connections with inclined screws

2.1 Theory and design

The load carrying capacity of joints with dowel-type fasteners can be determined by the different equations for the three failure modes based on Johansen´s yield theory. The load-carrying capacity for failure mode 1 is limited by the embedding strength of one or two timber members. For failure modes 2 and 3, the load-carrying capacity is limited by the embedding strength of the timber members and the bending capacity of the fastener. In failure mode 2 one plastic hinge and in failure mode 3 two plastic hinges per shear plane and fastener occur.

In order to determine the load-carrying capacity of timber-to-timber connections with inclined screws Johansen´s yield theory is extended. For this purpose, the withdrawal capacity of the screws, the angle between the screw axis and the force direction as well as the friction between the timber members are additional parameters influencing the load-carrying capacity. The friction resistance between the timber members is activated as soon as the joint is loaded since the contact surface between the timber members is loaded in compression. A timber-to-timber connection with inclined screws in shown in figure 1.

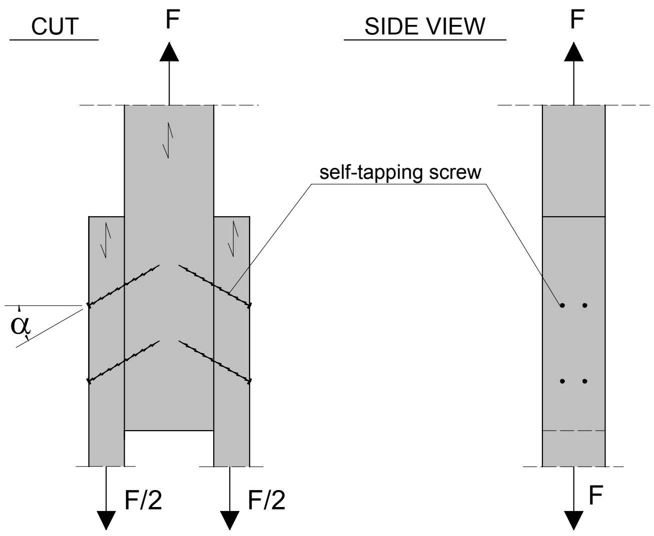

Figure 1: Timber-to-timber connection with inclined screws

One of the basic assumptions in Johansen´s yield theory is an ideal rigid-plastic material behaviour of the timber in embedding and of the fastener in bending. The withdrawal behaviour of screws, however, shows a clear maximum with a subsequent distinct load decrease. For the extension of Johansen's yield theory, the load-displacement behaviour of screws loaded in withdrawal therefore has to be taken into account. Depending on the axial displacement of the screw when reaching the ultimate load of the connection, the screw may or may not have reached its withdrawal capacity. The distribution of the shear stress along the length of the screw consequently has to be taken into account in the model. One possibility is to use a reduced withdrawal parameter taking into account the shear stress distribution along the screw length.

Using a reduced withdrawal parameter also allows to take into account the interaction between embedding and withdrawal strength of fasteners loaded parallel and perpendicular to the fastener axis. Since the distribution of the embedding stresses along the length of the fastener depends on the failure mode, also the modified withdrawal parameter $f_{1,mod}$ depends on the failure mode considered. The derivation of the different modified withdrawal capacity parameters is shown in paragraph 2.2.

In the following the extended design equation for Johansen´s failure mode 3 is derived (see figure 2). Basic assumptions are:

- Ideal rigid-plastic material behaviour for the timber under embedding stresses and of the fastener in bending.
- Averaged modified withdrawal parameters $f_{1,mod,i,j}$ for different failure modes considering the withdrawal behaviour depending on the lateral load. (see paragraph 2.2)

  i timber member (member 1 or 2)

  j Johansen´s failure mode (1a,l - 1a,r - 1b - 2a - 2b or 3)
- The angle or the inclination α is defined as the angle between the screw axis and the direction perpendicular to the grain.

For the notation see figure 2.

The following equations are based on the equilibrium in the undeformed state. If the deformed shape of the fastener is taken into account, the ultimate connection load increases.

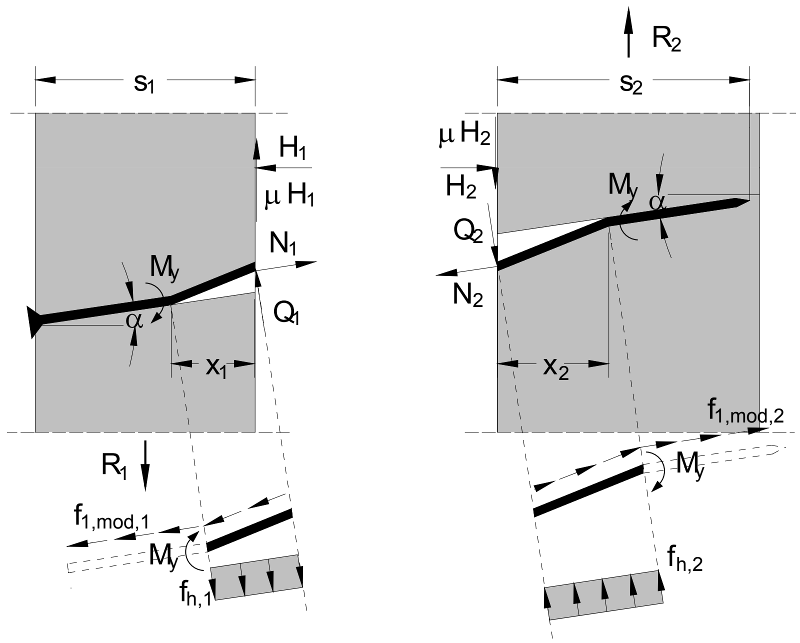

Figure 2: Forces and stresses in a timber-to-timber connection with an inclined screw for Johansen´s failure mode 3

The fastener bending moment in the interface between the timber members is:

$$M_1 = M_y - \frac{f_{h,1} \cdot d \cdot x_1^2}{2 \cdot \cos^2\alpha} \qquad \text{and} \qquad M_2 = -M_y + \frac{f_{h,2} \cdot d \cdot x_2^2}{2 \cdot \cos^2\alpha}$$

with $M_1 = M_2$ and $f_{h,2} = \beta \cdot f_{h,1}$ follows:

$$x_1^2 + \beta \cdot x_2^2 = \frac{4 \cdot M_y \cdot \cos^2\alpha}{d \cdot f_{h,1}} \tag{1}$$

Forces in the interface between the timber members:

$$R_1 = Q_1 \cdot \cos\alpha + N_1 \cdot \sin\alpha + \mu \cdot H_1 \tag{2a}$$

$$R_2 = Q_2 \cdot \cos\alpha + N_2 \cdot \sin\alpha + \mu \cdot H_2 \tag{2b}$$

$$H_1 = N_1 \cdot \cos\alpha - Q_1 \cdot \sin\alpha \tag{2c}$$

$$H_2 = N_2 \cdot \cos\alpha - Q_2 \cdot \sin\alpha \tag{2d}$$

with:

$$Q_1 = \frac{f_{h,1} \cdot d \cdot x_1}{\cos\alpha} \quad (3a) \qquad Q_2 = \frac{f_{h,2} \cdot d \cdot x_2}{\cos\alpha} \quad (3b)$$

$$N_1 = \frac{f_{1,mod,1} \cdot d \cdot s_1}{\cos\alpha} \quad (3c) \qquad N_2 = \frac{f_{1,mod,2} \cdot d \cdot s_2}{\cos\alpha} \quad (3d)$$

Substituting (3a), (3c) and (2c) in (2a) yields equation (4a):

$$R_1 = f_{1,mod,1} \cdot d \cdot s_1 \cdot (\mu + \tan\alpha) + f_{h,1} \cdot d \cdot (1 - \mu \cdot \tan\alpha) \cdot x_1 \tag{4a}$$

Similarly substituting (3b), (3d) and (2d) in (2b) yields equation (4b):

$$R_2 = f_{1,mod,2} \cdot d \cdot s_2 \cdot (\mu + \tan\alpha) + f_{h,2} \cdot d \cdot (1 - \mu \cdot \tan\alpha) \cdot x_2 \tag{4b}$$

Force equilibrium $R_1 = R_2$ results in equation (5):

$$\frac{(\mu + \tan\alpha)\cdot(f_{1,mod,1}\cdot s_1 - f_{1,mod,2}\cdot s_2)}{f_{h,1}\cdot(1-\mu\cdot\tan\alpha)} = \beta\cdot x_2 - x_1 \tag{5}$$

equating (1) and (5) yields equation (6):

$$x_1 = \frac{(\tan\alpha + \mu)\cdot(f_{1,mod,2}\cdot s_2 - f_{1,mod,1}\cdot s_1)}{(1-\mu\cdot\tan\alpha)\cdot f_{h,1}\cdot(1+\beta)} + \sqrt{\frac{2\cdot\beta}{1+\beta}}\cdot\sqrt{\frac{2\cdot M_y\cdot\cos^2\alpha}{f_{h,1}\cdot d} - \frac{(\tan\alpha+\mu)^2\cdot(f_{1,mod,1}\cdot s_1 - f_{1,mod,2}\cdot s_2)^2}{2\cdot f_{h,1}{}^2\cdot(1+\beta)\cdot(1-\mu\cdot\tan\alpha)^2}} \tag{6}$$

In addition to the force equilibrium $R_1 = R_2$, the compressive forces H_1 and H_2 in the contact surface between the timber members are equal: - (2c) = (2d) with (3a,b,c,d):

$$\frac{f_{1,mod,1}\cdot s_1 - f_{1,mod,2}\cdot s_2}{f_{h,1}\cdot\tan\alpha} = -\beta\cdot x_2 + x_1 \tag{7}$$

equating (7) with (5) yields equation (8):

$$-\frac{(f_{1,mod,1}\cdot s_1 - f_{1,mod,2}\cdot s_2)}{\tan\alpha} = \frac{(\mu+\tan\alpha)\cdot(f_{1,mod,1}\cdot s_1 - f_{1,mod,2}\cdot s_2)}{1-\mu\cdot\tan\alpha} \tag{8}$$

Equation (8) has only a solution for $f_{1,mod,1}\cdot s_1 = f_{1,mod,2}\cdot s_2$, since for $f_{1,mod,1}\cdot s_1 \neq f_{1,mod,2}\cdot s_2$ equation (8) results in $-1 = \tan^2\alpha$.

This means that the fastener tensile force in the left side timber member is equal to the tensile force in the right side timber member and the lower of the two fastener withdrawal capacities governs.

for $f_{1,mod,1}\cdot s_1 = f_{1,mod,2}\cdot s_2$ equation (6) may be modified to:

$$x_1 = \sqrt{\frac{2\cdot\beta}{1+\beta}}\cdot\sqrt{\frac{2\cdot M_y\cdot\cos^2\alpha}{f_{h,1}\cdot d}} \tag{9}$$

equation (9) in (4a):

$$R = f_{1,mod}\cdot d\cdot s\cdot(\mu+\tan\alpha) + (1-\mu\cdot\tan\alpha)\cdot\sqrt{\frac{2\cdot\beta}{1+\beta}}\cdot\sqrt{2\cdot M_y\cdot d\cdot f_{h,1}\cdot\cos^2\alpha} \tag{10}$$

The load-carrying capacity in timber-to-timber connections with inclined screws for Johansen´s extended failure mode 3 is then:

$$R_{VM3} = R_{ax,3}\cdot(\mu\cdot\cos\alpha + \sin\alpha) + (1-\mu\cdot\tan\alpha)\cdot\sqrt{\frac{2\cdot\beta}{1+\beta}}\cdot\sqrt{2\cdot M_y\cdot d\cdot f_{h,1}\cdot\cos^2\alpha} \tag{11}$$

with the withdrawal capacity $R_{ax,3}$ for Johansen´s failure mode 3:

$$R_{ax,3} = \min\left\{\begin{array}{l} f_{1,mod,1,3}\cdot d\cdot\dfrac{s_1}{\cos\alpha} \\ f_{1,mod,2,3}\cdot d\cdot\dfrac{s_2}{\cos\alpha}\end{array}\right\}$$

For timber-to-timber connections with screws arranged perpendicular to the grain ($\alpha \rightarrow 0°$), equation (11) results in equation (12):

$$R_{VM3,0°} = \mu \cdot R_{ax} + \sqrt{\frac{2 \cdot \beta}{1+\beta}} \cdot \sqrt{2 \cdot M_y \cdot d \cdot f_{h,1}} = \mu \cdot R_{ax} + R_{la,VM3} \qquad (12)$$

This equation for the load-carrying capacity in timber-to-timber connections with screws loaded perpendicular to their axis may also be found in the Draft German Timber Design Code E DIN 1052, Mai 2000 using a friction coefficient $\mu = 0{,}25$.

For the other failure modes the following equations are given:

$$R_{VM1a,l} = R_{ax,1al} \cdot \sin\alpha + f_{h,1} \cdot d \cdot s_1 \cdot \cos\alpha$$

$$R_{VM1a,r} = R_{ax,1ar} \cdot \sin\alpha + f_{h,2} \cdot d \cdot s_2 \cdot \cos\alpha$$

$$R_{VM1b} = R_{ax,1b} \cdot (\mu \cdot \cos\alpha + \sin\alpha)$$

$$+ \frac{f_{h,1} \cdot d \cdot s_1}{1+\beta} \cdot (1 - \mu \cdot \tan\alpha) \cdot \left[\sqrt{\beta + 2 \cdot \beta^2 \cdot \left[1 + \frac{s_2}{s_1} + \left(\frac{s_2}{s_1}\right)^2\right] + \beta^3 \cdot \left(\frac{s_2}{s_1}\right)^2} - \beta \cdot \left(1 + \frac{s_2}{s_1}\right)\right]$$

$$R_{VM2a} = R_{ax,2a} \cdot (\mu \cdot \cos\alpha + \sin\alpha)$$

$$+ (1 - \mu \cdot \tan\alpha) \cdot \frac{f_{h,1} \cdot s_1 \cdot d}{2+\beta} \cdot \left[\sqrt{2 \cdot \beta \cdot (1+\beta) + \frac{4 \cdot \beta \cdot (2+\beta) \cdot M_y \cdot \cos^2\alpha}{f_{h,1} \cdot d \cdot s_1^{\,2}}} - \beta\right]$$

$$R_{VM2b} = R_{ax,2b} \cdot (\mu \cdot \cos\alpha + \sin\alpha)$$

$$+ (1 - \mu \cdot \tan\alpha) \cdot \frac{f_{h,1} \cdot s_2 \cdot d}{1 + 2 \cdot \beta} \cdot \left[\sqrt{2 \cdot \beta^2 \cdot (1+\beta) + \frac{4 \cdot \beta \cdot (2 \cdot \beta + 1) \cdot M_y \cdot \cos^2\alpha}{f_{h,1} \cdot d \cdot s_2^{\,2}}} - \beta\right]$$

The load-carrying capacity in timber-to-timber connections with inclined screws is now:

$$R = \min\begin{Bmatrix} R_{VM1a,l} \\ R_{VM1a,r} \\ R_{VM1b} \\ R_{VM2a} \\ R_{VM2b} \\ R_{VM3} \end{Bmatrix} \qquad (13) \qquad\qquad R_{ax,j} = \min\begin{Bmatrix} f_{1,mod,1,j} \cdot d \cdot \dfrac{s_1}{\cos\alpha} \\ f_{1,mod,2,j} \cdot d \cdot \dfrac{s_2}{\cos\alpha} \end{Bmatrix} \qquad (14)$$

with j Johansen´s failure mode (failure mode 1a,l; 1a,r; 1b; 2a; 2b or 3)

2.2 Modified withdrawal capacity parameter

Equation (13) may be used to determine the load-carrying capacity of timber-to-timber connections with inclined screws. Johansen´s equations for the different failure modes were extended by the withdrawal capacity of the screws, the inclination angle of the screw axis as well as the friction between the timber members.

In order to establish the withdrawal contribution of the screw, the axial displacement Δ of the screw relative to the timber is determined, depending on the relative displacement δ

between the timber members in force direction. Figure 3 shows a timber-to-timber connection with an inclined screw and a total displacement between the timber members in force direction of $\delta_{tot} = \delta_1 + \delta_2$ for Johansen´s failure mode 3. It is assumed, that withdrawal failure only occurs in one timber member and the elongation of the screw is neglected. As shown in figure 3 point A is moving to point A*, if the screw is pulled out of the timber member 1. Otherwise point B is moving to point B*.

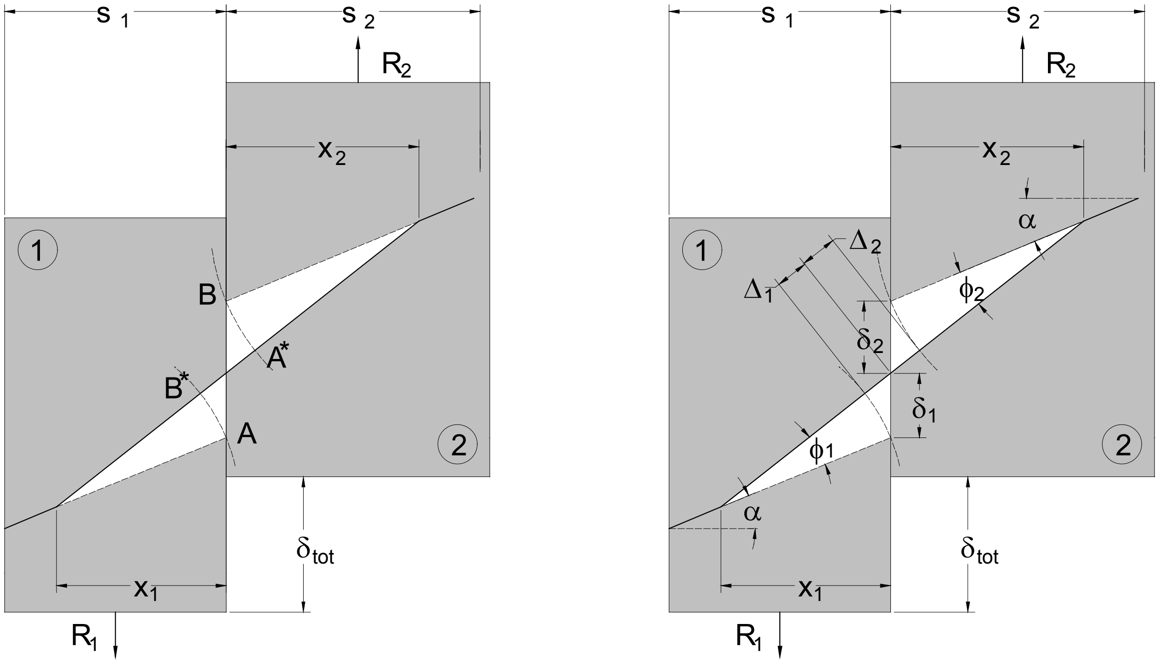

Figure 3: Displacements in a timber-to-timber connection with an inclined screw

For a relative displacement $\Delta_{tot} = \Delta_1 + \Delta_2$ parallel to the screw corresponding to the axial displacement at the ultimate withdrawal load, the ultimate load-carrying capacity of the timber-to-timber connection with inclined screws is reached. At this point the screw is pulled out of either the left or the right timber member.

for all failure modes the following applies (see figure 3):

$$\Delta_i = \frac{x_i}{\cos\alpha} \cdot \left(\left(\sqrt{\left(\frac{\delta_i}{x_i} + \tan\alpha \right)^2 + 1} \right) \cdot \cos\alpha - 1 \right) \qquad i = 1,2 \qquad (15)$$

with

$\phi_1 = \phi_2$ and $\delta_{tot} = \delta_1 + \delta_2$ and $\Delta_{tot} = \Delta_1 + \Delta_2$

follows

$$\Delta_{tot} = \frac{x_1 + x_2}{\cos\alpha} \cdot \left(\left(\sqrt{\left(\frac{\delta_{tot}}{x_1 + x_2} + \tan\alpha \right)^2 + 1} \right) \cdot \cos\alpha - 1 \right) \qquad (16)$$

The relative displacement between the timber members according to ISO 6891 is limited to $\delta_{max} = \delta_{tot} = 15$ mm.

The horizontal distance between the plastic hinge in the fastener and the interface between the timber members for Johansen´s failure mode 3 is (see also equation 9):

$$x_{1,VM3} = \sqrt{\frac{2 \cdot \beta}{1+\beta}} \cdot \sqrt{\frac{2 \cdot M_y \cdot \cos^2 \alpha}{f_{h,1} \cdot d}} \quad \text{and} \quad x_{2,VM3} = \frac{x_1}{\beta} \tag{17}$$

Average values for material properties of self-tapping screws determined in previous tests:

$$M_y = 500 \frac{N}{mm^2} \cdot \frac{d^3}{6} \quad \text{and} \quad f_h = 0{,}050 \cdot (1 - 0{,}01 \cdot d) \cdot \rho$$

Substituting (17) in equation (16) and using as an example the material properties determined in previous tests (ρ = 400 kg/m^3; $\beta = f_{h,2} / f_{h,1} = 1$) results for δ_{tot} = 15 mm in the relative axial displacement Δ_{tot} between the screw and the timber depending on the angle α and the screw diameter d for Johansen´s failure mode 3. The displacement Δ_{tot} for Johansen´s failure mode 3 is shown in figure 4.

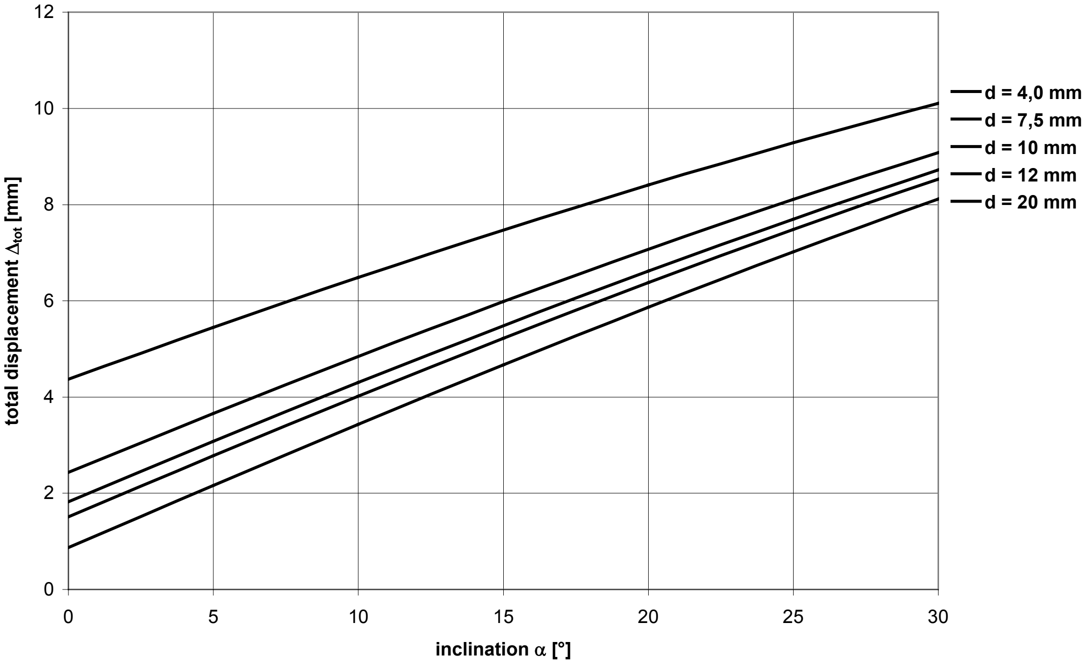

Figure 4: Δ_{tot} for δ_{tot} = 15 mm depending on α for Johansen´s failure mode 3

The total displacement Δ_{tot} for the remaining failure modes is determined by using the following expressions in equation (16):

$$x_{1,VM1b} = \frac{s_1}{2 \cdot (1+\beta)} \cdot \left[\sqrt{\beta + 2 \cdot \beta^2 \cdot \left[1 + \frac{s_2}{s_1} + \left(\frac{s_2}{s_1} \right)^2 \right] + \beta^3 \cdot \left(\frac{s_2}{s_1} \right)^2} + 1 - \beta \cdot \frac{s_2}{s_1} \right]$$

$$x_{2,VM1b} = \frac{\beta \cdot s_2 - s_1}{2 \cdot \beta} + \frac{x_1}{\beta}$$

$$x_{1,VM2a} = \frac{s_1}{2 \cdot (2+\beta)} \cdot \left[\sqrt{2 \cdot \beta \cdot (1+\beta) + \frac{4 \cdot \beta \cdot (2+\beta) \cdot M_y \cdot \cos^2 \alpha}{f_{h,1} \cdot d \cdot s_1^2}} + 2 \right]$$

$$x_{2,VM2a} = \frac{2 \cdot x_1 - s_1}{\beta}$$

$$x_{1,VM2b} = \frac{s_2}{1+2\cdot\beta}\cdot\left[\sqrt{2\cdot\beta^2\cdot(1+\beta)+\frac{4\cdot\beta\cdot(2\cdot\beta+1)\cdot M_y\cdot\cos^2\alpha}{f_{h,1}\cdot d\cdot s_2{}^2}}-\beta\right]$$

$$x_{2,VM2b} = \frac{1}{2\cdot\beta}\cdot\left[\beta\cdot s_2 + x_1\right]$$

With increasing inclination α the axial displacement Δ in a timber-to-timber connection increases for a fixed value of the connection displacement δ_{tot} = 15 mm. Due to the fact that the withdrawal capacity for screws in a withdrawal test is reached at a displacement of about 1,8 mm (see figure 5), the withdrawal capacity of screws with a diameter up to 8 mm is reached before a connection displacement δ of 15 mm is attained.

Typical withdrawal parameter-displacement curves for screws with a diameter d = 7,5 mm depending on different simultaneous embedding deformations are shown in figure 5. In the tests, the screw was loaded perpendicular to the axis until a prescribed embedding displacement was reached and subsequently pulled out of the timber while maintaining the embedding load. The withdrawal capacity for this diameter was reached at a maximum displacement of about 1,8 mm independent of the lateral displacement.

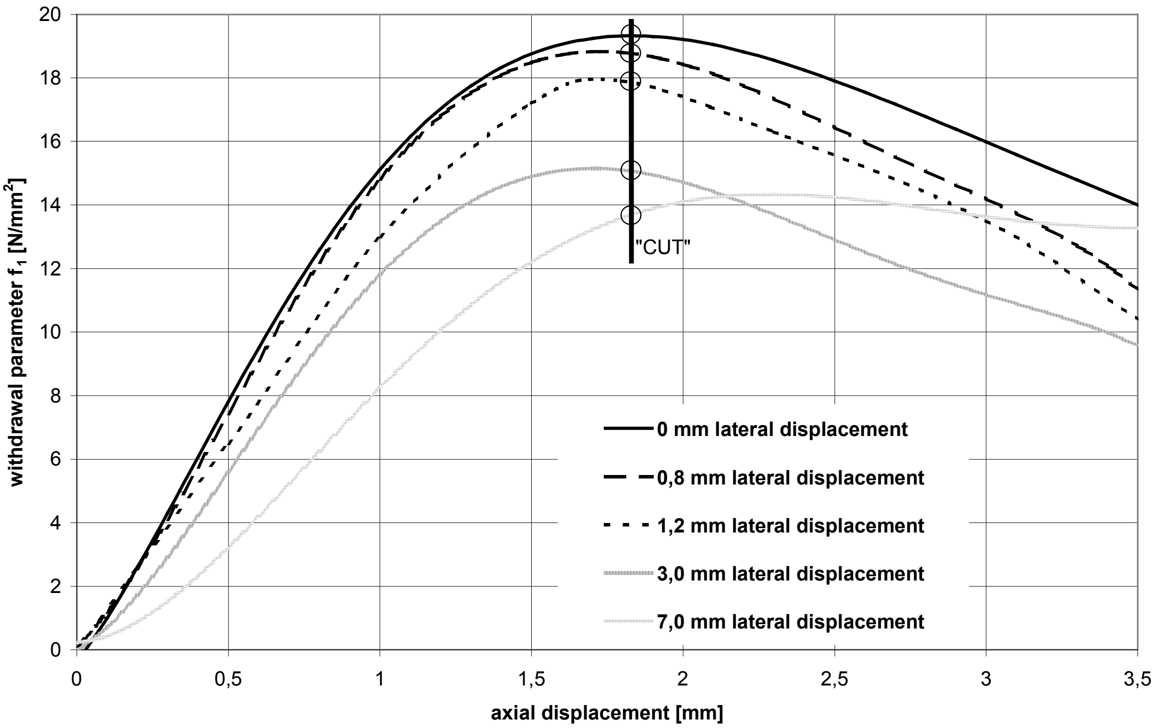

Figure 5: Typical withdrawal curves for screws with a diameter d = 7,5 mm for different lateral embedding displacements

Based on figure 5 the following observations are made:

- The withdrawal capacity is not reduced, as long as no plastic embedding deformation has taken place. This means that the full withdrawal capacity is available in those parts of the screw where the embedding strength is not reached (e.g. outside x_1 and x_2 in figure 3).
- The withdrawal capacity per unit length increases from the interface between the members towards the plastic hinge. The corresponding distribution of the withdrawal

capacity for an axial displacement of 1,8 mm is shown in figure 6, based on the values in figure 5.

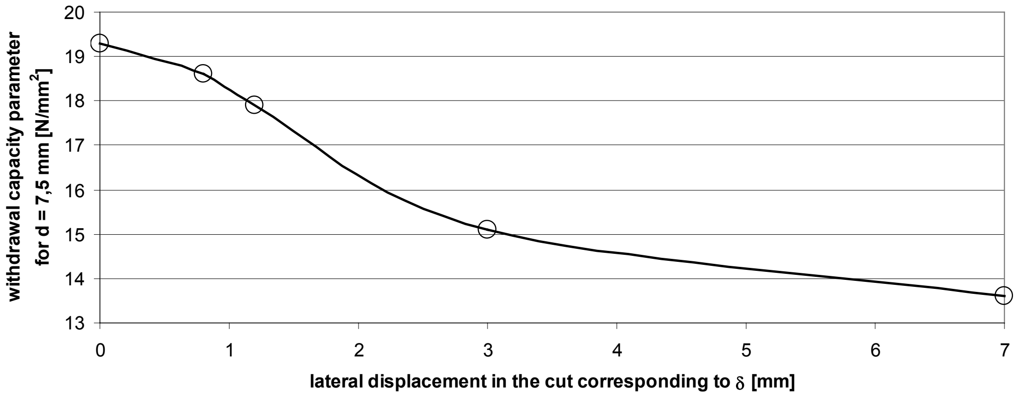

Figure 6: Withdrawal capacity parameter depending on lateral displacement for d = 7,5mm

Based on figure 6, the distribution of the local withdrawal capacity over the total member thickness is shown as a dashed line in figure 7. The solid line represents the modified withdrawal capacity parameter $f_{1,mod,1,3}$ or $f_{1,mod,2,3}$ for Johansen´s failure mode 3 as the mean value of the withdrawal capacity over the respective timber member thickness.

Similar withdrawal capacity parameter curves depending on the embedding deformation (see figure 6) and the resulting modified withdrawal capacity parameters (see figure 7) may be derived for the other failure modes based on the procedure described.

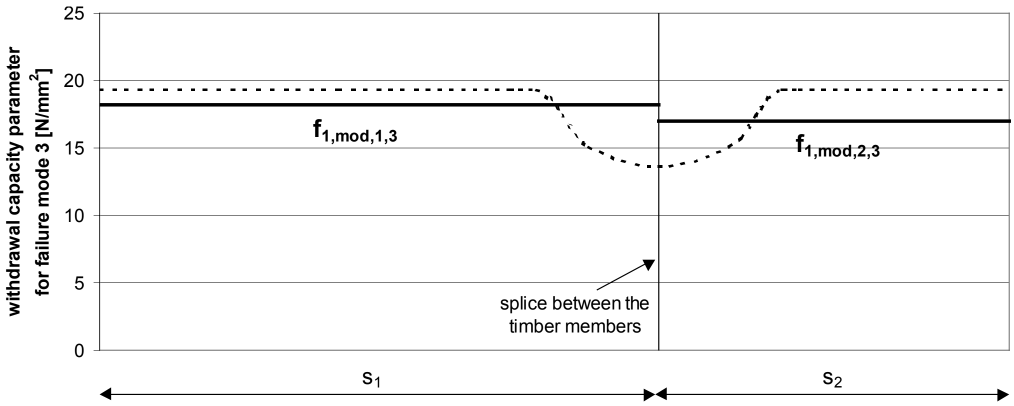

Figure 7: Modified withdrawal capacity parameter $f_{1,mod,1,3}$ or $f_{1,mod,2,3}$ for Johansen´s failure mode 3 for a screw diameter d = 7,5 mm in timber member 1 and 2

2.3 Comparison of model prediction and experimental data

Tests were made with specimens containing in each interface between the side and middle timber member either one self-tapping screw with continuous thread for series 1 or four self-tapping screws for series 2, see figure 1. The screw diameter was 7,5 mm and the screw length was 130 mm for series 1 and 180 mm for series 2.

The members were made of glued laminated timber beams with 12 % moisture content. All members within a specimen had similar density. The average density for joint members was 400 kg/m^3 for series 1 and 442 kg/m^3 for series 2.

Altogether nine sub-series (five sub-series for series 1 and four sub-series for series 2), respectively, were carried out whereby the angle α (0° until 50°) as well as the timber thickness and the penetration depth of the screw was varied.

The values of the load-carrying capacity per fastener and per shear plane reached in the tests is shown in figure 8. In this figure also the calculated load-carrying capacities per fastener and per shear plane based on the extended Johansen theory are shown. Parameters used for the calculated load-carrying capacities were determined in previous tests. Modified withdrawal capacity parameters $f_{1,mod,1,j}$ and $f_{1,mod,2,j}$ were determined as described in paragraph 2.2. In figure 9 the resulting modified withdrawal capacity parameters are shown for all failure modes and all angles α. A uniform value of the embedding strength was used, irrespective of the angle α.

For the timber-to-timber connections with an angle α of about 30°, the load-carrying capacity reached a maximum. This maximum was about 50 % higher than the value for screws arranged and loaded perpendicular to the fastener axis. Due to the decreasing penetration depth of the screws in the middle timber member with increasing angle for series 2, the load-carrying capacity for the timber-to-timber connections with an angle higher than 30° became smaller. The same observation was made in series 1 for an angle of 45° and a minimum penetration depth of about 32 mm. Here, the load-carrying capacity is higher for an inclination of 30° or 50°, where the penetration depth is larger.

An opened specimen with an inclination of 15° between the screw axis and the level direction is shown in figure 10. As expected, the connection failure was caused by reaching the withdrawal and bending capacity of the screw and the timber embedding strength (extended Failure Mode 3).

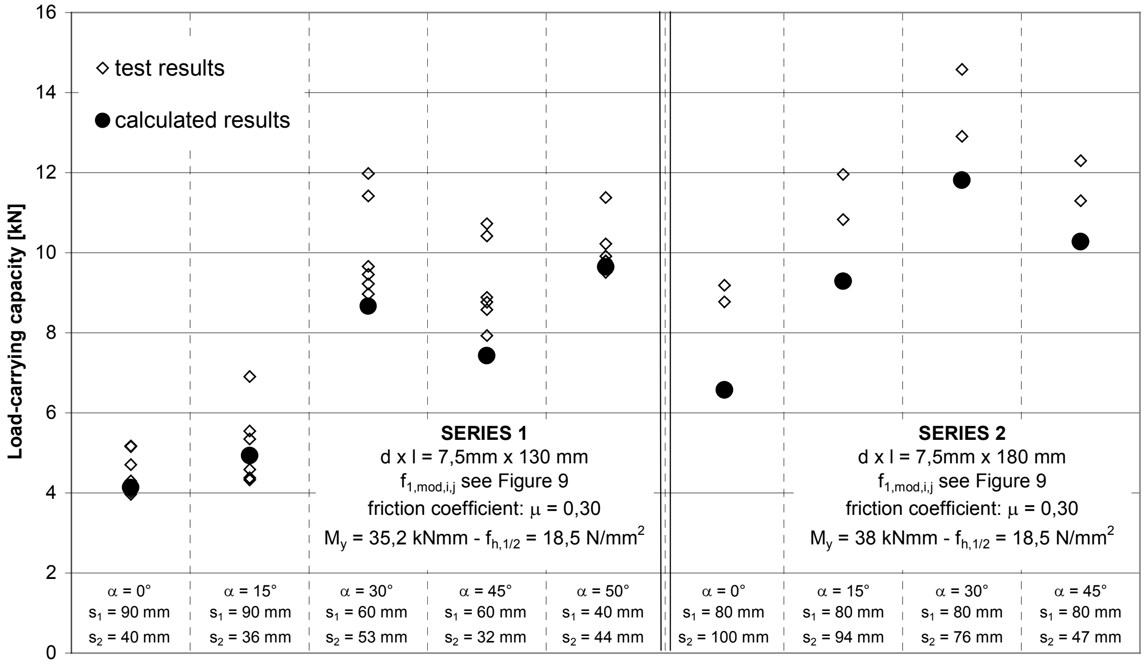

Figure 8: Comparison between test results and calculated load-carrying capacities

SERIES 1													
	failure mode 1a,l		failure mode 1a,r		failure mode 1b		failure mode 2a		failure mode 2b		failure mode 3		
α	$f_{1,mod,1,1al}$ [N/mm^2]	$f_{1,mod,2,1al}$ [N/mm^2]	$f_{1,mod,1,1ar}$ [N/mm^2]	$f_{1,mod,2,1ar}$ [N/mm^2]	$f_{1,mod,1,1b}$ [N/mm^2]	$f_{1,mod,2,1b}$ [N/mm^2]	$f_{1,mod,1,2a}$ [N/mm^2]	$f_{1,mod,2,2a}$ [N/mm^2]	$f_{1,mod,1,2b}$ [N/mm^2]	$f_{1,mod,2,2b}$ [N/mm^2]	$f_{1,mod,1,3}$ [N/mm^2]	$f_{1,mod,2,3}$ [N/mm^2]	**R [kN]**
0	13,6	19,3	19,3	13,6	15,1	15,7	15,1	16,3	18,7	16,6	18,6	17,7	**4,14**
15	14,6	19,3	19,3	14,6	17,4	17,9	17,3	18,0	19,0	17,6	18,9	18,2	**4,93**
30	15,5	19,3	19,3	15,5	18,2	18,3	18,1	18,9	19,0	18,1	18,9	18,9	**8,67**
45	16,5	19,3	19,3	16,5	18,4	18,7	18,3	18,8	19,1	18,4	19,1	18,9	**7,43**
50	17,4	19,3	19,3	17,4	18,6	18,6	18,4	19,1	19,0	18,4	19,0	19,0	**9,65**

SERIES 2													
	failure mode 1a,l		failure mode 1a,r		failure mode 1b		failure mode 2a		failure mode 2b		failure mode 3		
α	$f_{1,mod,1,1al}$ [N/mm^2]	$f_{1,mod,2,1al}$ [N/mm^2]	$f_{1,mod,1,1ar}$ [N/mm^2]	$f_{1,mod,2,1ar}$ [N/mm^2]	$f_{1,mod,1,1b}$ [N/mm^2]	$f_{1,mod,2,1b}$ [N/mm^2]	$f_{1,mod,1,2a}$ [N/mm^2]	$f_{1,mod,2,2a}$ [N/mm^2]	$f_{1,mod,1,2b}$ [N/mm^2]	$f_{1,mod,2,2b}$ [N/mm^2]	$f_{1,mod,1,3}$ [N/mm^2]	$f_{1,mod,2,3}$ [N/mm^2]	**R [kN]**
0	13,6	19,3	19,3	13,6	13,8	13,7	15,5	18,3	17,4	14,5	18,5	18,6	**6,58**
15	14,6	19,3	19,3	14,6	17,7	17,6	17,4	18,8	18,7	17,3	18,8	18,9	**9,29**
30	15,5	19,3	19,3	15,5	18,3	18,3	18,0	19,0	19,0	18,0	19,0	19,0	**11,8**
45	16,5	19,3	19,3	16,5	18,4	18,7	18,3	18,9	19,1	18,4	19,1	19,0	**10,3**

Figure 9: Modified withdrawal capacity parameters for all failure modes and all angles α

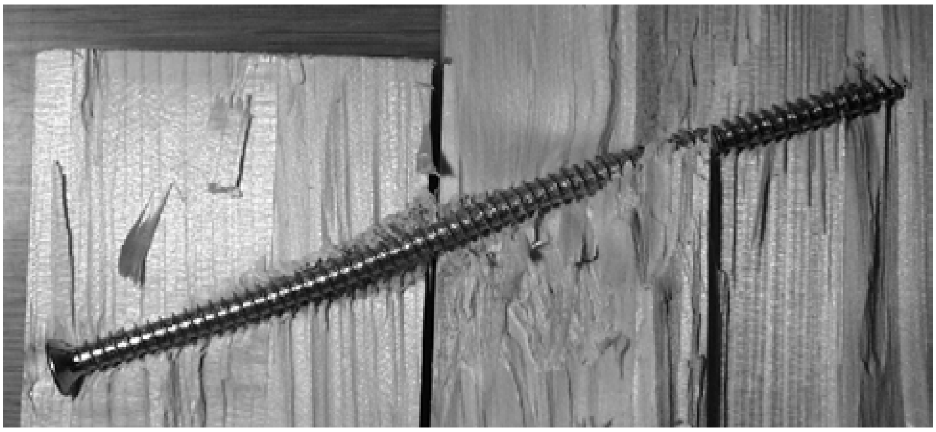

Figure 10: Opened specimen with self-tapping screw - Series 2 - $\alpha = 15°$

3 Conclusions

Inclined self-tapping screws provide opportunities for rationalisation and cost reduction in timber connections, particularly during design and installation. With the proposed equation (13), it is possible to determine the load-carrying capacity for all timber-to-timber connections with inclined screws taking into account the withdrawal and bending capacity of the screws, the timber embedding strength and the friction stress between the timber members. The withdrawal behaviour of the screws is taken into account in Johansen´s extended yield theory using a modified withdrawal capacity parameter.

Evaluating the modified withdrawal parameters for all screw diameters leads to the consequence, that screws with large diameters ($d > 8$ mm) do not reach their withdrawal capacity in a timber-to-timber connection for angles α close to 0° before a connection displacement of $\delta_{tot} = 15$ mm. Consequently, the modified withdrawal capacity parameters for $d > 8$ mm and $\alpha < 15°$ are much lower than the withdrawal capacity parameters determined in a withdrawal test. For these timber-to-timber connections the withdrawal action does not significantly increase the load-carrying capacity. However, for inclinations $\alpha > 30°$ the ultimate withdrawal capacity in a timber-to-timber connection is reached for all screw diameters.

For a general use of Johansen´s extended yield theory it is necessary to determine both, the modified withdrawal capacity parameters and the embedding strength depending on the angle between the screw axis and the grain direction for the different screw diameters.

To simplify the proposed design, the modified withdrawal capacity parameter $f_{1,mod,i,j}$ for timber member i and failure mode j may be determined as the minimum value $f_{1,mod,i,j} = 0,7 \cdot f_{1,i}$ (see figure 9) with the ultimate withdrawal capacity parameter $f_{1,i}$ from an axial withdrawal test for timber member i.

4 References

1. Blass, H.J., Bejtka, I., ´Standardisierung und Typisierung von Anschlüssen und Verbindungen zur Rationalisierung der Planung und Fertigung im Holz-Wohnhausbau - Teil A´ Forschungsbericht 2002, Versuchsanstalt für Stahl, Holz und Steine, Universität Karlsruhe (this research project was promoted by "Deutsche Gesellschaft für Holzforschung e.V. mit Mitteln des Bundesministeriums für Verkehr, Bau- und Wohnungswesen (Aktenzeichen: BS 34 - 5 80 01 98 - 18).
2. Blass, H.J., Bejtka, I, ´Screws with continuous threads in timber connections´,RILEM, Proceedings PRO 22, Stuttgart, Page 193
3. Blass, H.J., ´Verbindungen mit Nägeln und Schrauben - Bemessung nach E DIN 1052 und neuere Entwicklungen´, Ingenieurholzbau - Karlsruher Tage, September, 2000, 56-65
4. Ehlbeck, J., Ehrhardt, W., Screwed joints in ´Timber Engineering STEP 1, Basis of design, material properties, structural components and joints´ Centrum Hout, The Netherlands, ISBN 90-5645-001-8
5. Johansen, K.W., ´Theory of timber connections´ International Association of Bridge and Structural Engineering, Publication No. 9:249-262, Bern, Switzerland